Journal of Nuclear Medicine, published on September 30, 2021 as doi:10.2967/jnumed.121.262702

Predicting the outcome of epilepsy surgery by covariance pattern analysis of ictal perfusion SPECT

Jila Taherpour[1], Mariam Jaber[1], Berthold Voges[2], Ivayla Apostolova[1], Thomas Sauvigny[3], Patrick M. House[2], Michael Lanz[2], Matthias Lindenau[4], Susanne Klutmann[3], Tobias Martens[5], Stefan Stodieck[2], Ralph Buchert[1]

Departments of [1]Diagnostic and Interventional Radiology and Nuclear Medicine and [3]Neurosurgery, University Medical Center Hamburg-Eppendorf, 20246 Hamburg, Germany

[2]Department of Neurology and Epileptology, Protestant Hospital Alsterdorf, 22337 Hamburg, Germany

[4]Medical Practice Bredow & Partner, Neurology, 20354 Hamburg, Germany

[5]Department of Neurosurgery, Medical Center Asklepios St. Georg, 20099 Hamburg, Germany

Corresponding author: Ralph Buchert, Martinistr. 52, 20246 Hamburg, Germany, Email: r.buchert@uke.de, Phone: +49 40-7410-54347, Fax: +49 40-7410-40265, ORCID ID 0000-0002-0945-0724

First author: Jila Taherpour (resident), Martinistr. 52, 20246 Hamburg, Germany, Email: j.taherpour@uke.de , Phone: +49 1522-2832653, Fax: +49 40-7410-46767, ORCID ID 0000-0003-1247-752X

Word count: 4994

Short running title: Covariance analysis of ictal SPECT

ABSTRACT

Previous studies on the utility of specific perfusion patterns in ictal brain perfusion SPECT for predicting the outcome of temporal lobe epilepsy surgery used qualitative visual pattern classification, semi-quantitative region-of-interest analysis or conventional univariate voxel-based testing, which are limited by intra- and inter-rater variability and/or low sensitivity to capture functional interactions among brain regions. The present study performed covariance pattern analysis of ictal perfusion SPECT using the Scaled Subprofile Model for unbiased identification of predictive covariance patterns. **Methods:** The study retrospectively included 18 responders to temporal lobe epilepsy surgery (Engel I-A at 12 months follow-up) and 18 non-responders (≥ Engel I-B). Ictal SPECT images were analyzed with the Scaled Subprofile Model blinded to group membership for unbiased identification of the 16 covariance patterns explaining the highest proportion of variance in the whole data set. Individual expression scores of the covariance patterns were evaluated for predicting seizure freedom after temporal lobe surgery by ROC analysis. Kaplan-Meier analysis including all available follow-up data (up to 60 months after surgery) was also performed. **Results:** Amongst the 16 covariance patterns only one showed a different expression between responders and non-responders (P=0.03). This 'favorable ictal perfusion pattern' resembled the typical ictal perfusion pattern in temporomesial epilepsy. The expression score of the pattern provided an area of 0.744 (95%-confidence interval 0.577-0.911, P=0.004) under the ROC curve. Kaplan-Meier analysis revealed a statistical trend towards longer seizure freedom in patients with positive expression score (P=0.06). The median estimated seizure-free time was 48 months in patients with positive expression score versus 6 months in patients with negative expression score. **Conclusion:** The expression of the 'favorable ictal perfusion pattern' identified by covariance analysis of ictal brain perfusion SPECT provides

independent (from demographical and clinical variables) information for the prediction of seizure freedom after temporal lobe epilepsy surgery. The expression of this pattern is easily computed for new ictal SPECT images and, therefore, might be used to support the decision for or against temporal lobe surgery in clinical patient care.

Keywords: epilepsy; surgery; SPECT; ictal; covariance analysis

INTRODUCTION

Temporal lobe epilepsy (TLE) surgery fails to provide a major reduction in seizure frequency in a non-negligible fraction of patients with pharmacotherapy-refractory temporal lobe epilepsy (*1*). Furthermore, postoperative morbidity including psychiatric disorders, visual field defects, and cognitive impairment is observed in about 20% of the patients (*2*). Thus, there is a clinical need for additional preoperative predictors of surgical outcome to support the decision for or against TLE surgery in individual patients.

Ictal brain SPECT with ^{99m}Tc-labeled hexamethyl-propyleneamine oxime (^{99m}Tc-HMPAO) or ethyl cysteinate dimer (^{99m}Tc-ECD) is widely used to identify the seizure onset zone (SOZ) by regional hyperperfusion during the seizure. In patients with mesial TLE, ictal hyperperfusion typically involves the anteromesial temporal region as well as the anterolateral and inferior temporal neocortex (*3*,*4*). Other patterns with posterior extension of the ipsilateral temporal hyperperfusion, bitemporal hyperperfusion, more limited hyperperfusion in the ipsilateral temporal lobe or atypical patterns with hyperperfusion predominantly in other than anterotemporal brain regions have also been described in mesial TLE (*3*,*4*).

Previous studies on the utility of specific perfusion patterns in ictal brain perfusion SPECT for predicting the outcome of epilepsy surgery used qualitative visual classification of the ictal perfusion pattern (*4*), semi-quantitative region-of-interest analysis (*4*), or conventional voxel-based testing based on applying the same univariate statistical test and the same significance threshold at each single voxel of the SPECT image (*5*-*7*). Visual classification of ictal perfusion patterns is limited by intra- and interrater variability (*8*). The same is true for conventional voxel-based testing, since the interpretation of the resulting statistical maps is usually left to the

physician. Furthermore, relevant information in the ictal SPECT image might be missed by region-of-interest-based and conventional voxel-based analysis, when it does not reach the predefined significance threshold.

Against this background, the present study used Scaled Subprofile Model Principal Component Analysis (SSM-PCA) (*9-14*) for unbiased identification of covariance patterns for prediction of TLE surgery outcome from ictal perfusion SPECT.

MATERIALS AND METHODS

Patients for Covariance Pattern Analysis

We searched our database according to the following inclusion criteria: (I1) ictal SPECT with ^{99m}Tc-ECD or ^{99m}Tc-HMPAO for presurgical evaluation, (I2) age at ictal SPECT ≥16y, (I3) ictal tracer injection during a partial seizure, (I4) selective amygdalo-hippocampectomy or anteromedial temporal resection after ictal SPECT, and (I5) follow-up ≥12 months after surgery. These criteria were fulfilled by 65 patients. From these, patients were excluded if they met one or more of the following exclusion criteria: (E1) brain surgery prior to ictal SPECT or any other regional defect (*n*=8), (E2) no clear correlate of the seizure at ictal tracer injection in electroencephalography (EEG) (*n*=3), (E3) tracer injection during a secondarily generalized partial seizure (*n*=10), (E4) latency of the tracer injection after electrical seizure onset >60s (*n*=5), (E5) electrical seizure duration after tracer injection <20s (*n*=8), (E6) strong head motion during SPECT (*n*=1). This resulted in the exclusion of 29 patients. The remaining 36 patients were included in the covariance pattern analysis (44% females, median age at ictal SPECT

41.8y, interquartile range 24.9-47.7y). Ictal SPECT had been performed with ^{99m}Tc-ECD in 27 (75%) of these patients. ^{99m}Tc-HMPAO had been used in the remaining nine patients (25%).

The need for written informed consent was waived by the ethics review board of the general medical council of the state of Hamburg, Germany.

Perfusion SPECT

Tracer injection had been performed during video-EEG monitoring at all ictal injections. SPECT acquisition of 40min duration had been performed with a double-head camera (Siemens Symbia T2 or E.CAM) equipped with fanbeam or low-energy high-resolution collimators and angular steps of 2.8 or 3.0°. Projection data were retrieved from the archive for consistent retrospective image reconstruction: filtered backprojection with Butterworth filter of order 5 and cutoff 1.5 cycles/cm into transaxial SPECT slices with 3.9mm cubic voxels, Chang attenuation correction (μ=0.12/cm), no scatter correction, post-filtering with an isotropic Gaussian kernel with 8mm full-width-at-half-maximum.

Surgery

Twenty-six patients (14 responders, 12 non-responders) underwent selective amygdalo-hippocampectomy while the remaining ten patients (4 responders, 6 non-responders) had been submitted to anteromedial temporal resection. Surgery had been performed in the right hemisphere in 24 (67%) patients, in the left hemisphere in 12 (33%) patients.

Selective amygdalo-hippocampectomy was performed using a frontobasolateral transsylvian approach (*15*). After getting access to the M1 complex of the middle cerebral artery and the temporal branches, the mesial temporal structures were identified and subpial resection of the

uncal region and amygdala was performed. The hippocampal formation was removed en-bloc to the level of the midbrain tectum and submitted to neuropathological examination.

The anteromedial temporal resection was conducted via temporal craniotomy. The posterior limit of the neocortical resection was defined at about five centimeters from the temporal pole on the non-dominant hemisphere and four centimeters on the dominant hemisphere. The temporal pole was removed en block. Subsequently, the temporomesial structures (amygdala, hippocampus and parahippocampal gyrus) were removed to the level of the midbrain tectum. Temporal pole and hippocampal formation were submitted to neuropathological examination.

Follow-up

Postsurgical follow-up included at least one outpatient visit three to six months after surgery and at least one inpatient visit 12 months after surgery. The 12 months inpatient visit comprised detailed medical history, brain MRI, neuropsychological examination and three to four days video-EEG monitoring. Based on the complete data collected at these visits, the outcome at 12 months after surgery was categorized retrospectively according to the Engel Epilepsy Surgery Outcome Scale (*16*). The results are summarized in Fig. 1. For the covariance pattern analysis, the outcome at 12 months was dichotomized: patients with Engel I-A were considered 'responders' (n=18), all patients with Engel I-B or worse were considered 'non-responders' (n=18).

Clinical follow-up at 24, 36, 48 and 60 months was available in 14, 11, 11, and 10 responders, respectively (proportion of patients with Engel I-A: 86%, 82%, 73% and 70%). Clinical follow-up at 24, 36, 48 and 60 months was available in 15, 11, 9 and 6 non-responders (all Engel I-B or worse at all time points).

Image Preprocessing

Tracer-specific normal databases and templates in the Montreal Neurological Institute (MNI) space were generated as described in the Supporting Information.

Then, all individual SPECT images, including the 36 ictal SPECT and the 48 normal SPECT from the normal databases, were stereotactically normalized (affine) to MNI space using the statistical parametric mapping software package (SPM12) and the corresponding custom-made SPECT template. Stereotactically normalized SPECT were filtered with an isotropic Gaussian kernel with 15mm full-width-at-half-maximum and then scaled to the individual mean tracer uptake of the filtered image in a cerebrum parenchyma mask predefined in MNI space.

Voxel-wise mean, standard deviation and coefficient of variance were computed from the stereotactically normalized, filtered and scaled SPECT images, separately for the ^{99m}Tc-ECD and for the ^{99m}Tc-HMPAO normal database.

Individual stereotactically normalized, filtered and scaled ictal SPECT images were transformed voxel-wise to z-scores using the following formula: z-score=(individual tracer uptake–M)/SD, where M and SD are the mean value and the standard deviation of normal ^{99m}Tc-ECD or normal ^{99m}Tc-HMPAO uptake (depending on the tracer used in this subject) in the considered voxel.

Finally, ictal z-score images of the subjects in whom TLE surgery had been performed in the left hemisphere were left-right flipped at the mid-sagittal plane so that the right side was the site of surgery in all ictal z-score images.

Visual SPECT Interpretation

Visual interpretation of the ictal SPECT images was performed independently by two readers blinded to all other data. The readers first lateralized the SOZ based on regional hyperperfusion (left, right, both hemispheres, no hyperperfusion) and then localized the SOZ (temporal, frontal, parietal, occipital). In case of temporal hyperperfusion, additional hyperperfusion in ipsilateral insular cortex, basal ganglia and thalamus was considered to be a propagation effect that supports ipsilateral temporal seizure onset (*17*). Each reader interpreted all images twice. Images with discrepant interpretation with respect to lateralization and/or localization in the two reading sessions were assessed a third time to obtain an "intra-reader consensus". Finally, images with discrepant intra-reader consensus with respect to lateralization and/or localization between the two readers were assessed in a common reading session of the two readers to obtain an inter-reader consensus.

Conventional Univariate Voxel-based Analysis

Z-score maps of ictal SPECT were compared voxel-wise between responders and non-responders using the unpaired t-test model implemented in SPM12. The latency of the tracer injection after electrical seizure onset in EEG was taken into account as a covariate. The significance level was set at uncorrected P=0.005. Minimum cluster size was 1ml.

Identification of a Prognostic Covariance Pattern Analysis

Spatial covariance analysis of the ictal z-score images was performed with SSM-PCA implemented in the freely available Scan Analysis and Visualization Processor software package (version ScAnVP7.0w) (*10*). The covariance analysis was restricted to the same cerebrum

parenchyma mask that was used for intensity scaling in order to avoid truncation artefacts. The ictal z-score maps were not log-transformed for SSM-PCA in order to avoid truncation of negative z-scores. Negative z-scores indicate regional reduction of tracer uptake, which represents a relevant component of ictal perfusion patterns.

SSM-PCA with log-transformation was used to assess differences in normal cerebral uptake between ^{99m}Tc-ECD and ^{99m}Tc-HMPAO in the corresponding normal databases.

Statistical Analysis

Proportions are given as percentage and were compared between two groups using Fisher's exact test. Nominal variables with more than two possible values are given as percentages and were compared between groups using Pearson's Chi-Square test. Continuous variables are given as median and interquartile range and were compared using the non-parametric Mann-Whitney U test. All tests were two-sided. $P<0.05$ was considered significant.

The individual expression scores of the 16 covariance patterns identified by SSM-PCA in the ictal z-score images were compared between responders and non-responders using the unpaired t-test.

The prognostic power of the expression score of a given covariance pattern in ictal z-score images was assessed by ROC analysis. In addition, the expression score was dichotomized ('≤ 0' versus '> 0') and then tested as factor in Kaplan-Meier analysis of seizure freedom (Engel I-A) taking into account the total individual follow-up period. The log-rank test was used to compare the difference in seizure-free time for statistical significance.

Data Availability

All covariance patterns identified in this study are available upon request. Custom-made ^{99m}Tc-ECD and ^{99m}Tc-HMPAO templates as well as voxel-wise mean and standard deviation images of the ^{99m}Tc-ECD and ^{99m}Tc-HMPAO normal databases are also available upon request.

RESULTS

Demographical, clinical, ictal SPECT and surgery data of the 36 patients included in the SSM-PCA are summarized in Table 1. Responders and non-responders did not differ with respect to sex, age at ictal SPECT, age at first seizure, duration of disease, seizure frequency, and proportion of patients with impairment of awareness in the majority of seizures. Responders and non-responders also did not differ with respect to lateralization (relative to TLE surgery) of seizure semiology, interictal EEG, ictal EEG and MRI prior to ictal SPECT (Table 1). They also did not differ with respect to delay of surgery after ictal SPECT, side of resection and neuropathology of the surgical specimen (Table 1). The proportion of patients in whom ictal SPECT was performed with ^{99m}Tc-ECD was higher amongst the responders (94% versus 56%, P=0.02). The latency of tracer injection relative to the electrical seizure start was shorter in the responders (median 30s versus 40s, P=0.02). Tracer dose for ictal SPECT and electrical duration of the seizure after tracer injection did not differ between responders and non-responders.

^{99m}Tc-ECD and ^{99m}Tc-HMPAO SPECT templates generated from the normal databases are shown in Supplemental Fig. 1A. The voxel-wise coefficient of variance of the tracer uptake in the two normal databases is shown in Supplemental Fig. 1B. The first covariance pattern obtained by SSM-PCA of the 48 SPECT of the normal databases (Supplemental Fig. 2)

explained 28.2% of the total variance and was the only pattern with significantly different expression between the two tracer-specific normal databases ($P<0.001$; all other patterns: $P\geq0.15$).

Visual interpretation of the ictal SPECT identified the ipsilateral temporal lobe as SOZ in 12 (67%) responders and in 14 (78%) non-responders. Visual interpretation localized the SOZ in the contralateral temporal lobe in two responders (11%). Bilateral hyperperfusion was described in one responder (6%). None of the non-responders showed more pronounced contralateral or bilateral temporal hyperperfusion. The SOZ was localized to the temporal lobe in all patients with ictal hyperperfusion. No regional hyperperfusion was detected in three (17%) responders and in four (22%) non-responders. The differences in the visual lateralization of ictal SPECT between responders and non-responders were not significant ($P=0.35$).

The mean z-score maps of ictal SPECT are shown in Fig. 2. The statistical parametric maps obtained by voxel-based statistical comparison of the z-score maps between responders and non-responders revealed higher z-scores (more pronounced hyperperfusion) in responders in the contralateral (relative to resection) temporal and occipital lobe (Fig. 3A). There was a small cluster of lower z-scores (more pronounced hypoperfusion) in responders in the mesial frontal lobe (mainly ipsilateral, Fig. 3A).

Amongst the 16 covariance patterns determined by SSM-PCA in the 36 ictal SPECT only one, the ‘favorable ictal perfusion pattern’ (FIPP), showed different expression between responders and non-responders ($P=0.03$, Fig. 3B; all other patterns: $P\geq0.10$). The individual expression score of the FIPP provided an area of 0.744 (95%-confidence interval 0.577-0.911, $P=0.004$) under the ROC curve for the differentiation of responders from non-responders (Fig. 4A). Kaplan-Meier analysis revealed a statistical trend towards longer seizure freedom in

patients with positive FIPP expression score compared to patients with negative FIPP expression score (P=0.06, Fig. 4B). The median estimated seizure-free time was 48 months (positive expression score) versus 6 months (negative expression score).

DISCUSSION

This study used SSM-PCA to identify a covariance pattern (FIPP) in ictal brain perfusion SPECT whose expression is predictive of seizure freedom after TLE surgery. The FIPP expression score is easily computed for new ictal SPECT images to support their interpretation with respect to the chance of the patient to become seizure-free by TLE surgery. The computation is fully automatic and, therefore, does not require special expertise, in contrast to visual interpretation of ictal SPECT images.

SSM-PCA is stable with respect to variable image characteristics associated with the use of different scanners for image acquisition and/or different software for image preprocessing (*18*). This simplifies widespread clinical use. We hypothesize that the FIPP identified in this mono-site study is useful also for other sites.

The FIPP comprises more pronounced ictal hyperperfusion in the anterior part of the ipsilateral (to resection) temporal lobe, less pronounced posterior extension of the ictal hyperperfusion in the ipsilateral temporal lobe, hyperperfusion in the contralateral temporal lobe (less pronounced than ipsilateral), hypoperfusion in the precuneus/posterior cingulate cortex area and in the ipsilateral parietotemporal region, and more pronounced hypoperfusion in the anterior frontal lobe (Fig. 3B). The FIPP resembles the typical perfusion pattern during complex partial seizures in patients with mesial TLE (*4,19-22*). Pronounced ictal hyperperfusion in the anterior

ipsilateral temporal lobe is the most consistent finding in ictal perfusion SPECT in mesial temporal epilepsy (*3*,*23*). The lack of this pointer is a known risk factor of worse TLE surgery outcome (*4*). Hyperperfusion beyond the ipsilateral mesial temporal lobe might be explained by seizure propagation (*24*,*25*) and/or intrinsic epileptogenicity of the hyperperfused areas beyond the mesial temporal lobe. The FIPP suggests that hyperperfusion in the contralateral temporal lobe is predictive of good outcome of TLE surgery and, therefore, most likely is due to seizure propagation via interhemispheric connections. A 'SPECT mirror image' defined as ictal hyperperfusion contralateral to the seizure onset that is rather symmetrical to the ipsilateral ictal hyperperfusion is observed in ≥50% of epilepsy patients (*26*). The SSM-PCA was blinded not only to group membership (responders versus non-responders) but also to the results of visual interpretation and univariate voxel-based analysis. Thus, all images were handled equally by the SSM-PCA. In particular, no difference was made between ictal SPECT with or without mirror image. The aim of SSM-PCA is fully unbiased identification of the covariance patterns explaining the highest proportion of variance in the whole data set reflecting between- and within-group differences with the same accuracy (*9*).

Ictal hyperperfusion was stronger in the contralateral than in the ipsilateral temporal lobe in two (11%) responders so that visual interpretation suggested the contralateral temporal lobe as SOZ (Supplemental Fig. 3). Both subjects were seizure-free for ≥36 months after surgery. The FIPP expression score was borderline in both. Incorrect lateralization by visual interpretation of ictal perfusion SPECT in 5-8% of patients with mesialtemporal epilepsy has been described previously (*4*,*26*-*28*).

None of the tested demographical, clinical and surgical variables showed a statistically significant difference between the responders and the non-responders in this study (Table 1).

This suggests that the FIPP expression score provides independent prognostic information beyond these variables.

In clinical routine, visual evaluation and univariate voxel-based analysis of ictal perfusion SPECT are usually restricted to the localization of the SOZ. Classification of ictal perfusion patterns (beyond SOZ localization) for predicting surgery outcome is not common in clinical routine. On the other hand, the FIPP expression score alone is not useful for SOZ localization. Thus, visual analysis supported by univariate voxel-based analysis and SSM-PCA are complementary methods.

The following limitations of this study should be noted. First, the latency of tracer injection relative to the electrical seizure start differed between responders and non-responders. Ictal perfusion patterns are dynamic and, therefore, depend on the injection time (*19*). In order to account for this, the latency of the tracer injection was taken into account as covariate in the conventional univariate voxel-based analysis, although the difference was rather small (median latency 10s shorter in responders compared to non-responders). The fact that the resulting statistical map (Fig. 3A) is compatible with the FIPP (Fig. 3B) suggests that a potential effect of the injection latency on the FIPP is small. Furthermore, variability of the z-score maps associated with between-subjects variability of the injection latency might have been captured by one (or more) covariance patterns without affecting the FIPP. Second, the FIPP was derived from z-score images and therefore might not be applicable to SPECT uptake images. The transformation to z-scores was used to allow pooling of ^{99m}Tc-ECD and ^{99m}Tc-HMPAO SPECT. SSM-PCA of the uptake images in the ^{99m}Tc-ECD subsample confirmed the major findings of SSM-PCA of the z-score images in the whole sample (section “Identification of a prognostic covariance pattern in the ^{99m}Tc-ECD subsample” (*13*) including Supplemental Tab. 1 and Supplemental

Figs. 4,5 in the Supporting Information). It also outperformed region-of-interest based analyses (section "Region-of-interest based prediction in the ^{99m}Tc-ECD subsample" and Supplemental Fig. 6 in the Supporting Information). SSM-PCA might also be applied directly to pooled uptake images, which probably would result in one (or more) covariance patterns covering the regional differences in tracer uptake between ^{99m}Tc-ECD and ^{99m}Tc-HMPAO. Third, rather restrictive eligibility criteria were employed in this study. The use of the FIPP expression score should be restricted to ictal perfusion SPECT that fulfil the same criteria. For example, patients with brain surgery prior to ictal perfusion SPECT or any other major defect in tracer uptake (e.g., due to a stroke) should be excluded, because the defect might have a relevant impact on the FIPP expression score. Further studies should evaluate the FIPP expression score in independent patient samples and compare it with visual classification by experienced readers.

CONCLUSION

This study identified a covariance pattern in ictal perfusion SPECT whose expression provided independent information for the prediction of complete seizure freedom after temporal lobe epilepsy surgery. This favorable ictal perfusion pattern (FIPP) resembled the typical ictal perfusion pattern in mesial temporal epilepsy. The expression of the FIPP is easily computed for new ictal SPECT images and, therefore, might be used to support the decision for or against temporal lobe epilepsy surgery in clinical patient care.

Financial disclosure: None of the authors has any conflict of interest to disclose.

KEY POINTS

QUESTION: This study used the Scaled Subprofile Model for unbiased identification of a covariance pattern in ictal brain perfusion SPECT for predicting the outcome of temporal lobe epilepsy surgery.

PERTINENT FINDINGS: The identified ‘favorable ictal perfusion pattern’ resembled the typical ictal perfusion pattern in temporomesial epilepsy. The expression score of the pattern provided an area of 0.744 (95%-confidence interval 0.577-0.911, P=0.004) under the ROC curve for predicting seizure freedom 12 months after surgery.

IMPLICATIONS FOR PATIENT CARE: The expression score of the ‘favorable ictal perfusion pattern’ is easily computed automatically for new ictal SPECT images and, therefore, might be used to support the decision for or against temporal lobe epilepsy surgery in clinical patient care.

REFERENCES

1. West S, Nevitt SJ, Cotton J, et al. Surgery for epilepsy. *Cochrane Database Syst Rev.* 2019;6:CD010541.

2. Brotis AG, Giannis T, Kapsalaki E, Dardiotis E, Fountas KN. Complications after Anterior Temporal Lobectomy for Medically Intractable Epilepsy: A Systematic Review and Meta-Analysis. *Stereotact Funct Neurosurg.* 2019;97:69-82.

3. Ho SS, Berkovic SF, McKay WJ, Kalnins RM, Bladin PF. Temporal lobe epilepsy subtypes: differential patterns of cerebral perfusion on ictal SPECT. *Epilepsia.* 1996;37:788-795.

4. Ho SS, Newton MR, McIntosh AM, et al. Perfusion patterns during temporal lobe seizures: relationship to surgical outcome. *Brain.* 1997;120:1921-1928.

5. Apostolova I, Tast C, Wilke F, Lindenau M, Buchert R. Ictal perfusion SPECT in presurgical epilepsy diagnosis: Prognostic value of perfusion pattern for outcome of amygdalahippocampectomy [abstract]. *J Nucl Med.* 2010;51(suppl 2):1798.

6. Tast C. *Iktuale Perfusions-SPECT in der prächirurgischen EpilepsieDiagnostik: Explorative Analyse der Befundmuster hinsichtlich prognostischer Relevanz*. MD thesis, Hamburg: Department of Nuclear Medicine, University Medical Center Hamburg-Eppendorf, University Hamburg; 2012.

7. Kazemi NJ, Worrell GA, Stead SM, et al. Ictal SPECT statistical parametric mapping in temporal lobe epilepsy surgery. *Neurology.* 2010;74:70-76.

8. Lee HW, Hong SB, Tae WS. Opposite ictal perfusion patterns of subtracted SPECT. Hyperperfusion and hypoperfusion. *Brain.* 2000;123:2150-2159.

9. Alexander GE, Moeller JR. Application of the scaled subprofile model to functional imaging in neuropsychiatric disorders: A principal component approach to modeling brain function in disease. *Hum Brain Mapp.* 1994;2:1-16.

10. Eidelberg D. Metabolic brain networks in neurodegenerative disorders: a functional imaging approach. *Trends Neurosci.* 2009;32:548-557.

11. Moeller JR, Strother SC, Sidtis JJ, Rottenberg DA. Scaled subprofile model: a statistical approach to the analysis of functional patterns in positron emission tomographic data. *J Cereb Blood Flow Metab.* 1987;7:649-658.

12. Spetsieris P, Ma Y, Peng S, et al. Identification of disease-related spatial covariance patterns using neuroimaging data. *J Vis Exp.* 2013;76:e50319.

13. Spetsieris PG, Eidelberg D. Scaled subprofile modeling of resting state imaging data in Parkinson's disease: methodological issues. *Neuroimage.* 2011;54:2899-2914.

14. Moeller JR, Strother SC. A regional covariance approach to the analysis of functional patterns in positron emission tomographic data. *J Cereb Blood Flow Metab.* 1991;11:A121-135.

15. Yasargil MG, Teddy PJ, Roth P. Selective amygdalo-hippocampectomy. Operative anatomy and surgical technique. *Adv Tech Stand Neurosurg.* 1985;12:93-123.

16. Engel J. Outcome with respect to epileptic seizures. In: Engel J, ed. *Surgical Treatment of the Epilepsies*. New York: Raven Press; 1987:553-571

17. Dupont P, Zaknun JJ, Maes A, et al. Dynamic perfusion patterns in temporal lobe epilepsy. *Eur J Nucl Med Mol Imaging.* 2009;36:823-830.

18. Peng S, Ma Y, Spetsieris PG, et al. Characterization of disease-related covariance topographies with SSMPCA toolbox: effects of spatial normalization and PET scanners. *Hum Brain Mapp.* 2014;35:1801-1814.

19. Dupont P, Zaknun JJ, Maes A, et al. Dynamic perfusion patterns in temporal lobe epilepsy. *Eur J Nucl Med Mol Imaging.* 2009;36:823-830.

20. Blumenfeld H, McNally KA, Vanderhill SD, et al. Positive and negative network correlations in temporal lobe epilepsy. *Cereb Cortex.* 2004;14:892-902.

21. Tae WS, Joo EY, Kim JH, et al. Cerebral perfusion changes in mesial temporal lobe epilepsy: SPM analysis of ictal and interictal SPECT. *Neuroimage.* 2005;24:101-110.

22. Van Paesschen W, Dupont P, Van Driel G, Van Billoen H, Maes A. SPECT perfusion changes during complex partial seizures in patients with hippocampal sclerosis. *Brain.* 2003;126:1103-1111.

23. Kim BJ, Hong SB, Seo DW. Differences in ictal hyperperfusion of limbic-related structures between mesial temporal and neocortical epilepsy. *Epilepsy Res.* 2008;81:167-175.

24. Connors BW, Pinto DJ, Telfeian AE. Local pathways of seizure propagation in neocortex. *Int Rev Neurobiol.* 2001;45:527-546.

25. Jenssen S, Roberts CM, Gracely EJ, Dlugos DJ, Sperling MR. Focal seizure propagation in the intracranial EEG. *Epilepsy Res.* 2011;93:25-32.

26. Huberfeld G, Habert MO, Clemenceau S, Maksud P, Baulac M, Adam C. Ictal brain hyperperfusion contralateral to seizure onset: the SPECT mirror image. *Epilepsia.* 2006;47:123-133.

27. Lee SK, Lee SH, Kim SK, Lee DS, Kim H. The clinical usefulness of ictal SPECT in temporal lobe epilepsy: the lateralization of seizure focus and correlation with EEG. *Epilepsia.* 2000;41:955-962.

28. Wichert-Ana L, Velasco TR, Terra-Bustamante VC, et al. Typical and atypical perfusion patterns in periictal SPECT of patients with unilateral temporal lobe epilepsy. *Epilepsia.* 2001;42:660-666.

FIGURES

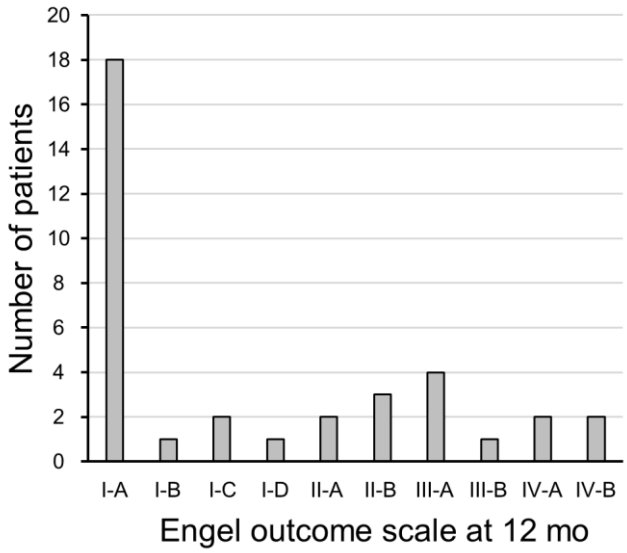

FIGURE 1 Engel Epilepsy Surgery Outcome Scale at 12 months after temporal lobe epilepsy surgery. Patients with Engel I-A at 12 months were considered responders, all other patients were considered non-responders.

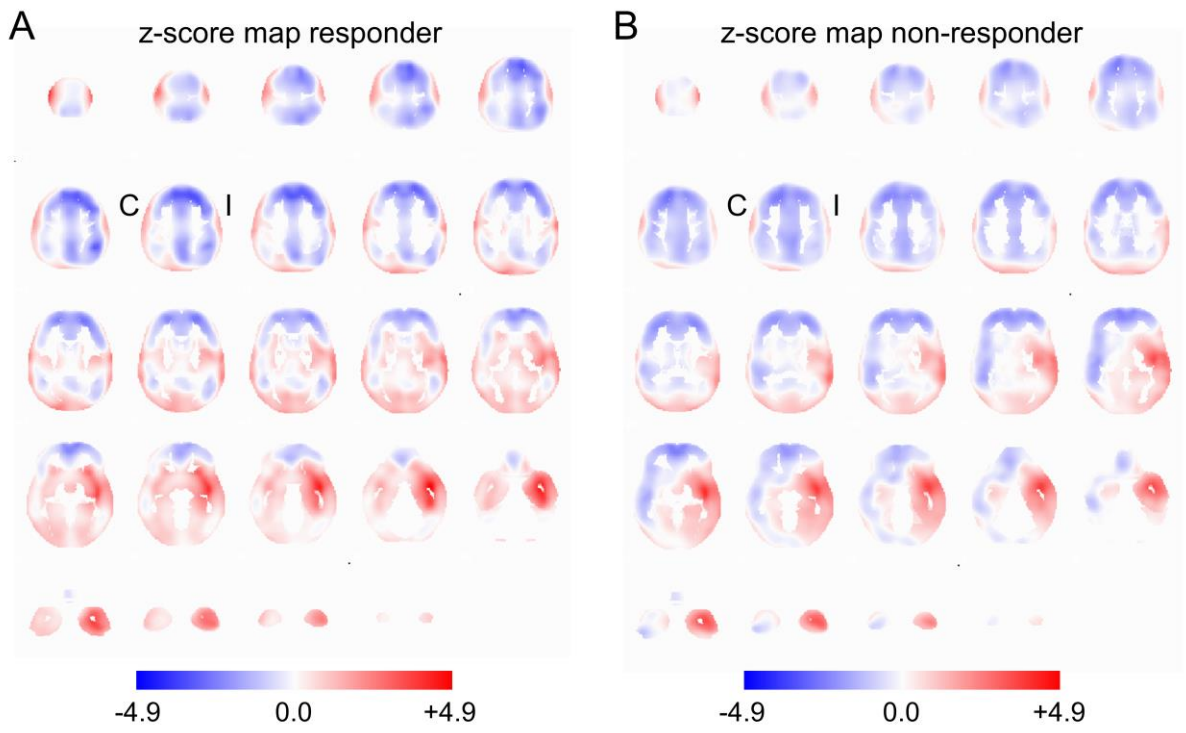

FIGURE 2 Mean z-score maps of ictal SPECT in the 18 responders (**A**) and in the 18 non-responders (**B**) in MNI space. Positive z-scores (red) indicate increased perfusion (relative to the custom-made normal databases), negative z-scores (blue) indicate reduced perfusion. (I / C = Ipsilateral / Contralateral to temporal lobe epilepsy surgery)

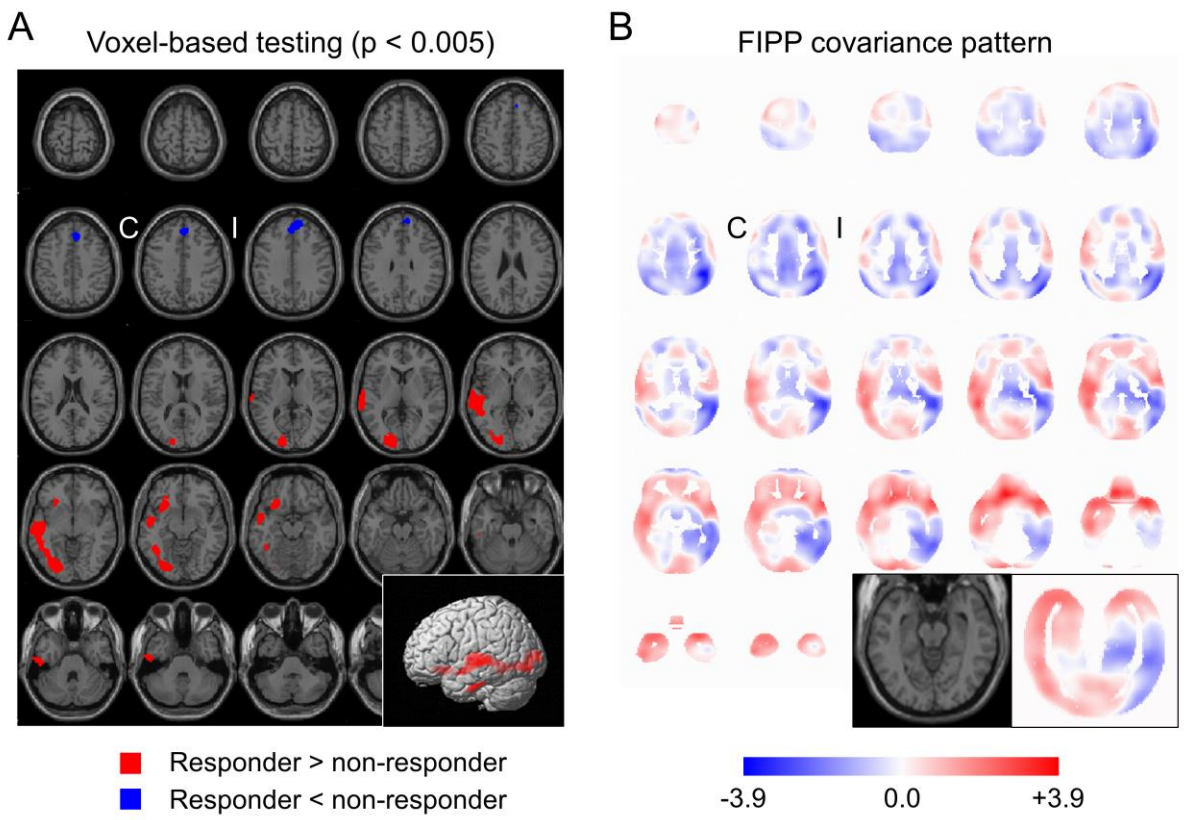

FIGURE 3 Statistical maps of hyperperfusion (red) and hypoperfusion (blue) obtained by conventional univariate voxel-based one-sided t-tests corrected for injection latency, thresholded at *P*=0.005 and overlaid to the SPM single subject template (**A**). Part **B** shows the 'favorable ictal perfusion pattern' (FIPP). (I / C = Ipsilateral / Contralateral to temporal lobe epilepsy surgery).

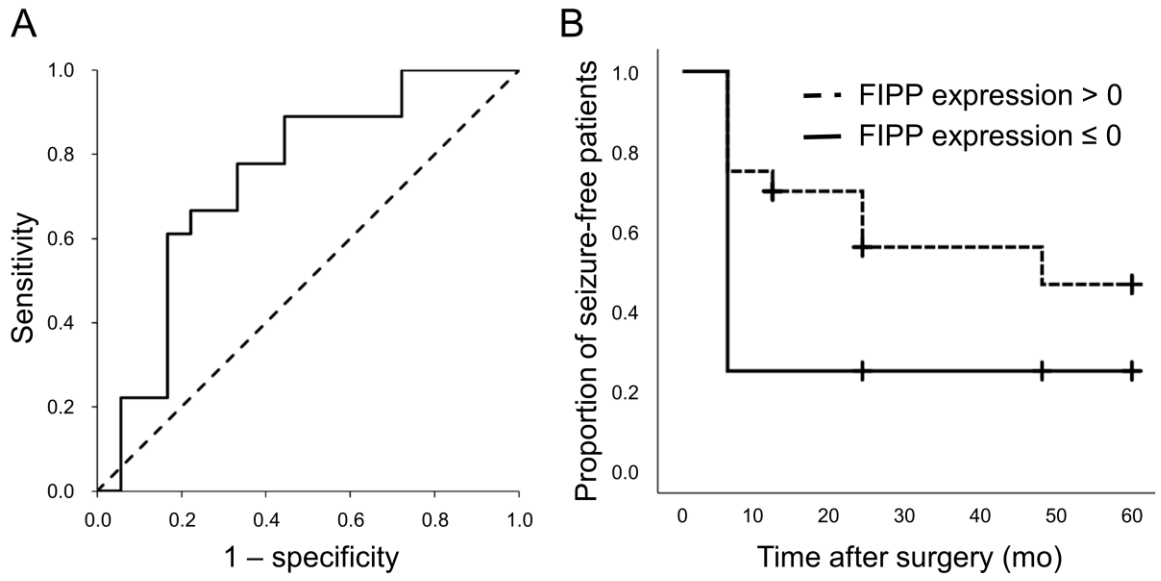

FIGURE 4 ROC analysis of the FIPP expression score for identification of responders (**A**), and Kaplan-Meier analysis of patients with positive FIPP expression score versus patients with negative FIPP expression score (**B**).

TABLE 1 Demographical, clinical, SPECT and surgical data.

	responder*	non-responder*	*P*†
number of patients	18	18	
sex [% females]	44	44	1.00
age at ictal SPECT [y]	43 [28-49]	34 [24-48]	0.24
age at first seizure [y]	14 [6-23]	12 [4-23]	0.61
duration of disease at SPECT [y]	22 [15-34]	21 [11-33]	0.56
mean seizure frequency in the last 12 months before ictal SPECT [seizures/month]	5 [3-21] (*n*=15)	14 [5-23] (*n*=16)	0.36
with impairment of awareness in the majority of seizures during the last 12 months [%]	77 (*n*=13)	79 (*n*=14)	1.00
lateralization of seizure semiology: ipsilateral to resection/contralateral/both/no [%]	93/7/0/0 (*n*=14)	90/0/0/10 (*n*=10)	0.35
lateralization of MRI: ipsilateral to resection/contralateral/both/no [%]	94/0/0/6 (*n*=18)	82/0/6/12 (*n*=17)	0.45
lateralization of ictal EEG prior to ictal SPECT: ipsilateral to resection/contralateral/both/no [%]	88/6/6/0 (*n*=16)	88/0/0/12 (*n*=17)	0.26
lateralization of interictal EEG prior to ictal SPECT: ipsilateral to resection/contralateral/both/no [%]	83/6/11/0	67/0/22/11	0.26
tracer of ictal SPECT [% 99mTc-ECD]	94	56	0.02
tracer activity administered for ictal SPECT [MBq]	524 [479-639]	578 [501-632]	0.34
latency of tracer injection to seizure start in EEG [s]	30 [25-35]	40 [30-49]	0.02
seizure duration after injection according to EEG [s]	74 [43-147]	57 [31-106]	0.28
delay of surgery after ictal SPECT [months]	10 [4-27]	6 [2-24]	0.70
side of TLE surgery [% right]	67	67	1.00
neuropathology of surgical specimen: normal/sclerosis/mass lesion/focal cortical dysplasia	13/75/6/6 (*n*=16)	17/67/17/0 (*n*=12)	0.66

*Continuous variables are given as median [interquartile range]. If a variable was not available in all patients, the number of patients for that variable is given in parentheses.

†The *P*-values are not corrected for multiple testing.

Graphical Abstract

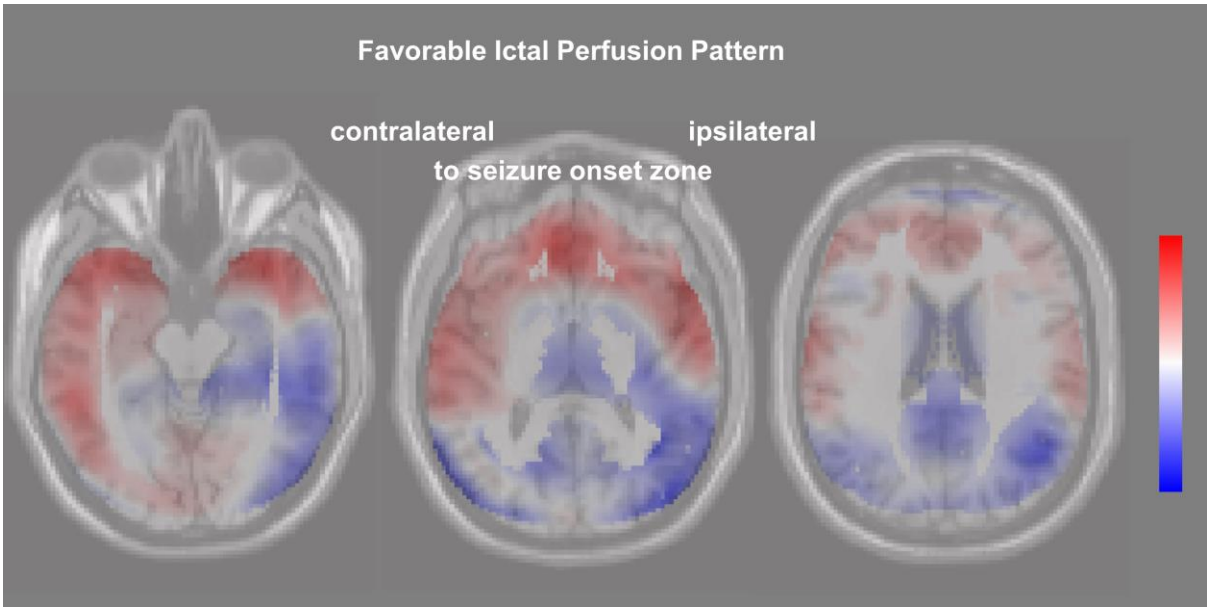

Supporting Information

Predicting the outcome of epilepsy surgery by covariance pattern analysis of ictal perfusion SPECT

Jila Taherpour[1] (ORCID ID 0000-0003-1247-752X), Mariam Jaber[1], Berthold Voges[2], Ivayla Apostolova[1], Thomas Sauvigny[3], Patrick M. House[2], Michael Lanz[2], Matthias Lindenau[4], Susanne Klutmann[3], Tobias Martens[5], Stefan Stodieck[2], Ralph Buchert[1] (ORCID ID 0000-0002-0945-0724)

[1]Department of Diagnostic and Interventional Radiology and Nuclear Medicine, University Medical Center Hamburg-Eppendorf, 20246 Hamburg, Germany

[2]Department of Neurology and Epileptology, Protestant Hospital Alsterdorf, 22337 Hamburg, Germany

[3]Department of Neurosurgery, University Medical Center Hamburg-Eppendorf, 20246 Hamburg, Germany

[4]Medical Practice Bredow & Partner, Neurology, 20354 Hamburg, Germany

[5]Department of Neurosurgery, Medical Center Asklepios St. Georg, 20099 Hamburg, Germany

Normal databases

The database of the Department of Nuclear Medicine of the University Medical Center Hamburg-Eppendorf was searched for interictal brain perfusion SPECT with ^{99m}Tc-ECD or ^{99m}Tc-HMPAO that had been performed for presurgical evaluation of epilepsy patients but showed normal cerebral perfusion according to retrospective visual inspection. The identified brain SPECT images were further analyzed by voxel-based statistical testing (as described in subsection "Conventional univariate voxel-based analysis" in the manuscript) using a leave-one-out approach, separately for ^{99m}Tc-ECD and ^{99m}Tc-HMPAO. SPECT images with suspicious clusters of increased or decreased tracer uptake were excluded. The remaining interictal SPECT were included in the normal databases (^{99m}Tc-ECD: n=15, 40% females, median age = 30.4y, interquartile range = 23.7-39.5y; ^{99m}Tc-HMPAO: n=33, 48% females, median age = 33.6y, interquartile range = 24.3-43.8y; Chi-square test of sex: P=0.76, Mann-Whitney U test of age: P=0.69).

The majority of interictal SPECT included in the normal databases were from different patients than the ictal SPECT included in the covariance pattern analysis (except six interictal ^{99m}Tc-ECD SPECT and one interictal ^{99m}Tc-HMPAO SPECT).

SPECT templates

The SPECT images of the two normal databases were stereotactically normalized (affine transformation) to the anatomical space of the Montreal Neurological Institute (MNI) using the statistical parametric mapping software package (version SPM12) and the SPM SPECT template as target. For intensity scaling, stereotactically normalized images were divided voxel-by-voxel by the individual mean tracer uptake in a binary mask of the cerebrum parenchyma predefined in

MNI space. The ^{99m}Tc-ECD and the ^{99m}Tc-HMPAO SPECT template were obtained by voxel-based averaging of the scaled and stereotactically normalized SPECT images of the ^{99m}Tc-ECD and the ^{99m}Tc-HMPAO SPECT normal database, respectively.

Identification of a prognostic covariance pattern in the ^{99m}Tc-ECD subsample

The transformation of uptake images to z-scores images was used to allow pooling of ^{99m}Tc-ECD and ^{99m}Tc-HMPAO SPECT for the Scaled Subprofile Model Principal Component Analysis (SSM-PCA) in the whole patient sample described in the manuscript. Transformation to z-scores is the standard procedure to aid combined analysis of variables measured on different scales. However, transformation to z-scores most likely did not fully eliminate tracer effects, because scaling to z-scores only standardizes mean values and standard deviations, but it does not account for other possible differences (in higher moments such as skewness) of the distributions.

The SSM-PCA therefore was repeated in the subsample of patients in whom brain perfusion SPECT had been performed with ^{99m}Tc-ECD (17 responders, 10 non-responders). Demographical, clinical, ictal SPECT and surgery data of these patients are summarized in Supplemental Tab. 1. Responders and non-responders with ictal ^{99m}Tc-ECD SPECT did not differ with respect to sex, age at ictal SPECT, age at first seizure, duration of disease at ictal SPECT, mean monthly seizure frequency in the last 12 months before ictal SPECT, and the proportion of patients with impairment of awareness in the majority of seizures in the last 12 months before ictal SPECT. Responders and non-responders also did not differ with respect to lateralization (relative to the brain hemisphere of temporal lobe epilepsy surgery) of seizure semiology, interictal EEG, ictal EEG and MRI prior to ictal SPECT (Supplemental Tab. 1). They also did not differ with respect to the ^{99m}Tc-ECD activity dose administered for ictal SPECT, the latency of tracer injection relative to the start of

the seizure in EEG, the electrical duration of the seizure after ^{99m}Tc-ECD injection, the delay of surgery after ictal ^{99m}Tc-ECD SPECT, the side of resection and the neuropathology of the surgical specimen (Supplemental Tab. 1). However, it should be noted that the statistical power for the detection of differences between responders and non-responders was smaller in the ^{99m}Tc-ECD subsample compared to the whole sample due to smaller and unbalanced (with respect to responders versus non-responders) sample sizes.

Spatial covariance analysis with SSM-PCA was applied to the stereotactically normalized ^{99m}Tc-ECD SPECT uptake images filtered with an isotropic Gaussian kernel with 15mm full-width-at-half-maximum and scaled to the individual mean tracer uptake of the filtered uptake image in the cerebrum parenchyma mask (rather than to z-score images as in the covariance analysis of ^{99m}Tc-ECD and ^{99m}Tc-HMPAO combined). The covariance analysis was restricted to the cerebrum parenchyma mask in order to avoid truncation artefacts. The SPECT images were log-transformed for SSM-PCA in order to optimize the detection of relevant effects (*1*).

Amongst the 16 covariance patterns determined by SSM-PCA again only one, the 'favorable ictal perfusion pattern with ^{99m}Tc-ECD' (ECD-FIPP), showed different expression between responders and non-responders (P=0.002, Supplemental Fig. 4; all other patterns: $P \geq 0.15$). The individual expression score of the ECD-FIPP provided an area of 0.859 (95%-confidence interval 0.713-1.000, P=0.002) under the ROC curve for the differentiation of responders from non-responders (Supplemental Fig. 5A). Kaplan-Meier analysis revealed significantly longer seizure freedom in patients with positive ECD-FIPP expression score compared to patients with negative ECD-FIPP expression score (P=0.04, Supplemental Fig. 5B). The median estimated seizure-free time was 48 months (positive expression score) versus 6 months (negative expression score).

The ECD-FIPP shared almost all major features with the FIPP including less pronounced posterior extension of the ictal hyperperfusion in the ipsilateral (to surgical resection) temporal lobe, hyperperfusion in the contralateral temporal lobe (more pronounced in the anterior part and with less pronounced posterior extension), hypoperfusion in the bilateral parietal lobe, and more pronounced hypoperfusion in the anterior frontal lobe (Supplemental Fig. 4). The only major difference was less versus more pronounced ictal hyperperfusion in the anterior part of the ipsilateral temporal lobe in the ECD-FIPP versus the FIPP (inserts in Supplemental Fig. 4). This difference between the two covariance patterns might be related to the fact that the anterior temporal lobe is amongst the brain regions with the largest difference of normal uptake between ^{99m}Tc-ECD and ^{99m}Tc-HMPAO (lower for ^{99m}Tc-ECD; insert in Supplemental Fig. 2). Minor differences between the ECD-FIPP and the FIPP might be explained by the fact that the ECD-FIPP was derived from uptake images whereas the FIPP was derived from z-score images.

Region-of-interest based prediction in the ^{99m}Tc-ECD subsample

The ECD-FIPP was dichotomized voxel-by-voxel at zero weight. This resulted in two regions-of-interest (ROI): “positive ECD-FIPP weights” and “negative ECD-FIPP weights”. The mean scaled ^{99m}Tc-ECD uptake was computed for each of the two ROIs for each of the 27 ^{99m}Tc-ECD SPECT. The performance of two ROI averages for the discrimination between responders and non-responders was tested by ROC analysis.

The area under the ROC curve of the mean ^{99m}Tc-ECD uptake was larger for the “positive ECD-FIPP weights”-ROI (0.803, 95%-confidence interval 0.639-0.967) than for the “negative ECD-FIPP weights”-ROI (0.685, 0.470-0.901). However, the ^{99m}Tc-ECD uptake in the “positive ECD-FIPP weights”-ROI was outperformed by the ECD-FIPP expression score by more than 5%

(area under the ROC curve 0.859 versus 0.803; Supplemental Fig. 6) suggesting that the ECD-FIPP expression score is superior for predicting the outcome of temporal lobe epilepsy surgery. This might be explained by the fact that SSM-PCA more likely covers the full spatial extent of the relevant perfusion changes throughout the whole brain in ictal perfusion SPECT than conventional ROI analysis.

Supplemental References

1. Spetsieris PG, Eidelberg D. Scaled subprofile modeling of resting state imaging data in Parkinson's disease: methodological issues. Neuroimage. 2011;54:2899-2914.

Supplemental Figures

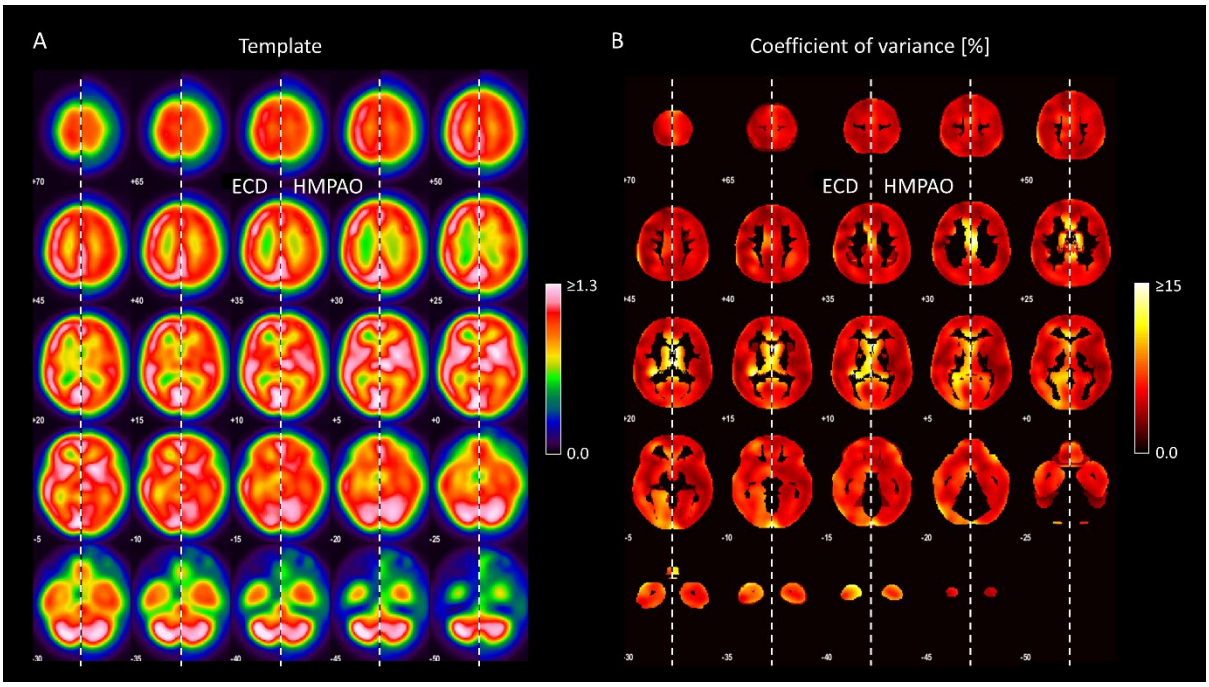

SUPPLEMENTAL FIGURE 1 Custom-made template (**A**) and voxelwise coefficient of variance (**B**) of ^{99m}Tc-ECD and ^{99m}Tc-HMPAO SPECT in MNI space. In each slice, the left half presents ^{99m}Tc-ECD, the right half presents ^{99m}Tc-HMPAO.

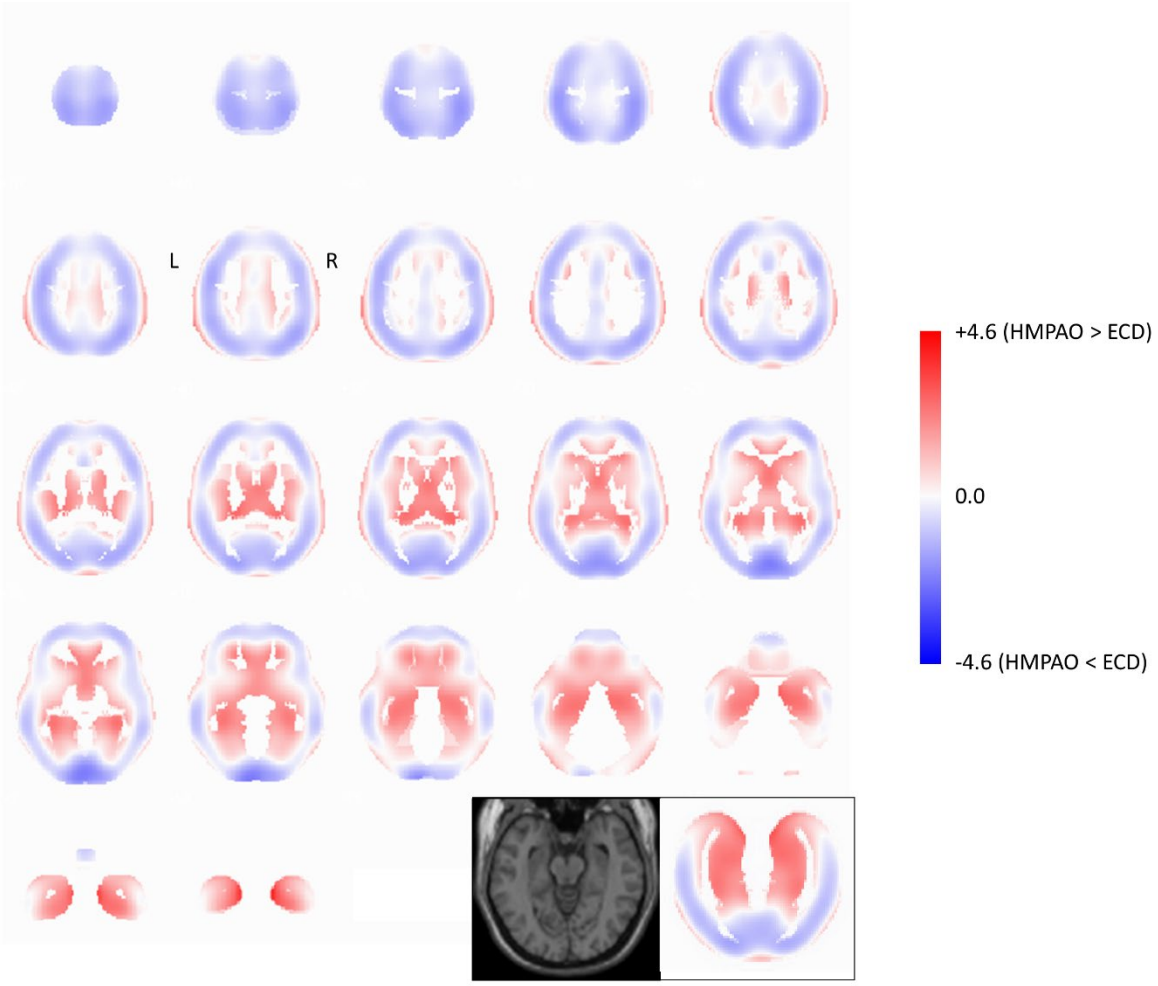

SUPPLEMENTAL FIGURE 2 Tracer covariance pattern identified by SSM-PCA applied to all SPECT images in the ^{99m}Tc-ECD and in the ^{99m}TC-HMPAO normal database combined. SSM-PCA was blinded for the tracer. Positive intensity (red) indicates relatively higher uptake of ^{99m}TC-HMPAO, negative intensity (blue) indicates relatively higher uptake of ^{99m}Tc-ECD. The insert on the bottom right shows a slice of the tracer covariance pattern along the longitudinal axes of the temporal lobes.

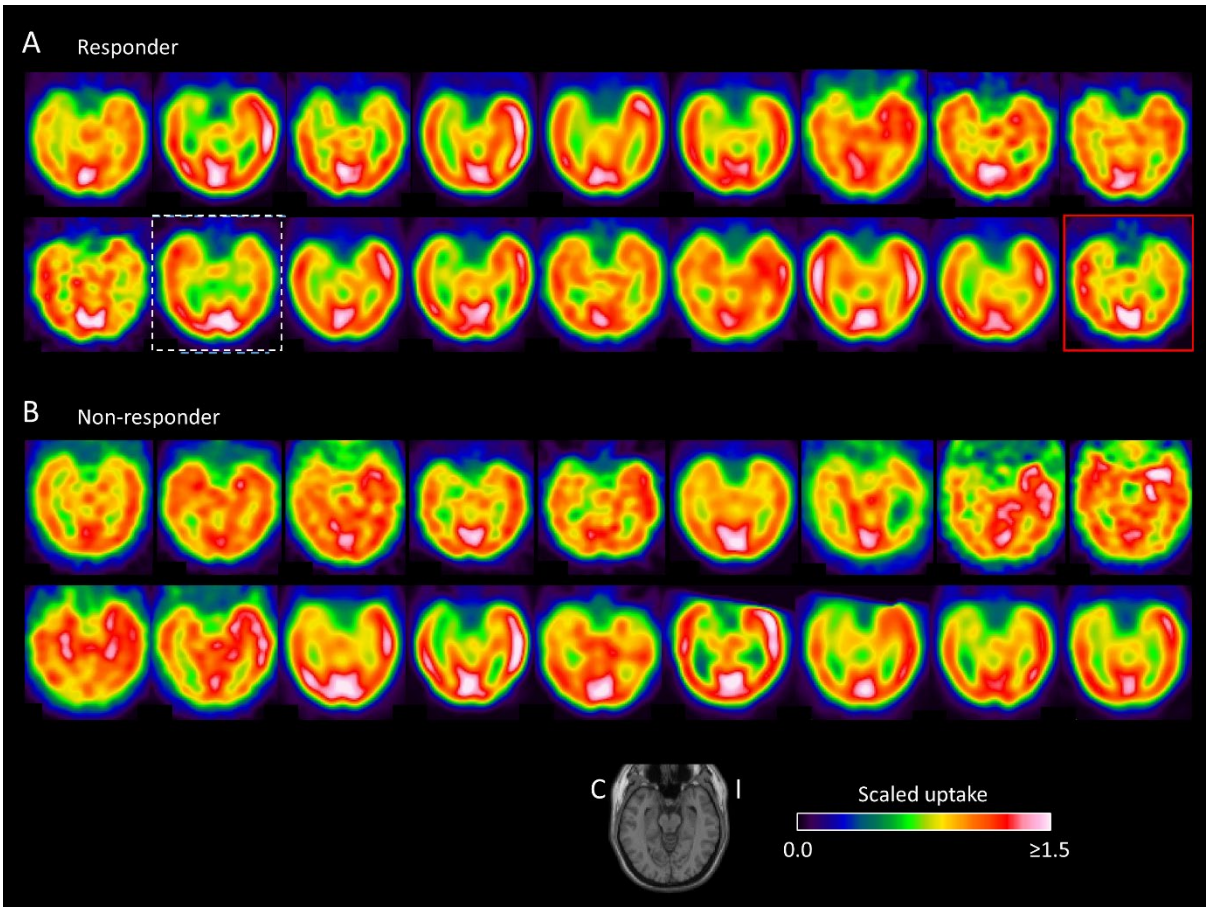

SUPPLEMENTAL FIGURE 3 Scaled uptake images of ictal perfusion SPECT in the 18 responders (**A**) and in the 18 non-responders (**B**) (I / C = Ipsilateral / Contralateral to temporal lobe epilepsy surgery). The same central slice parallel to the longitudinal axes of the temporal lobes is shown for each patient. The boxes label the two responders in whom visual interpretation lateralized the seizure onset zone contralateral to the temporal lobe epilepsy surgery. Both patients presented a borderline FIPP expression score (white dashed box: slightly negative, red continuous box: slightly positive). Both patients were free of seizures (Engel I-A) for 36 months after surgery. The patient in the white dashed box continued to be seizure free during the whole available follow-up of 60 months. The patient in the red continuous box was classified as Engel I-B at the 48 months and at the 60 months follow-up.

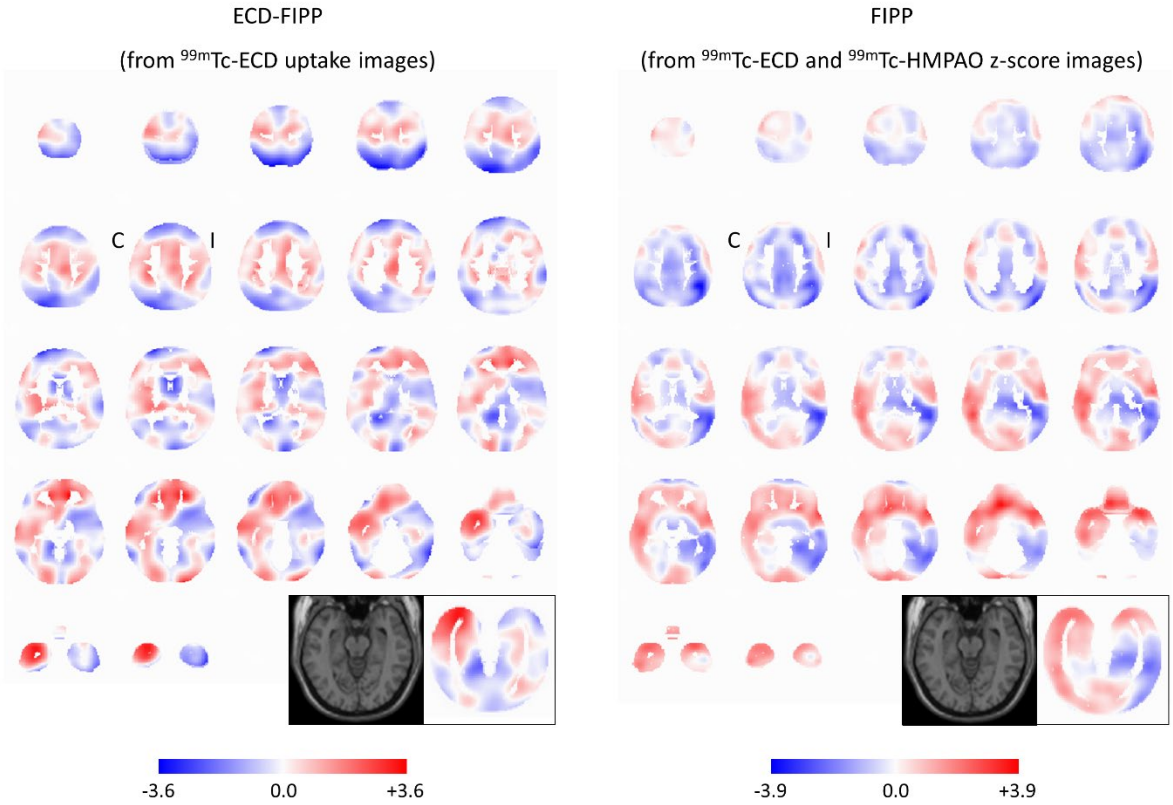

SUPPLEMENTAL FIGURE 4 'Favorable ictal perfusion pattern with ^{99m}Tc-ECD' (ECD-FIPP) derived from ^{99m}Tc-ECD uptake images in MNI space (left). The 'favorable ictal perfusion pattern' (FIPP) derived from z-score images of ^{99m}Tc-ECD and ^{99m}Tc-HMPAO combined (taken from Fig. 3B in the manuscript) is shown for comparison. The inserts show the same slice of the two covariance patterns along the longitudinal axes of the temporal lobes. (I / C = Ipsilateral / Contralateral to temporal lobe epilepsy surgery)

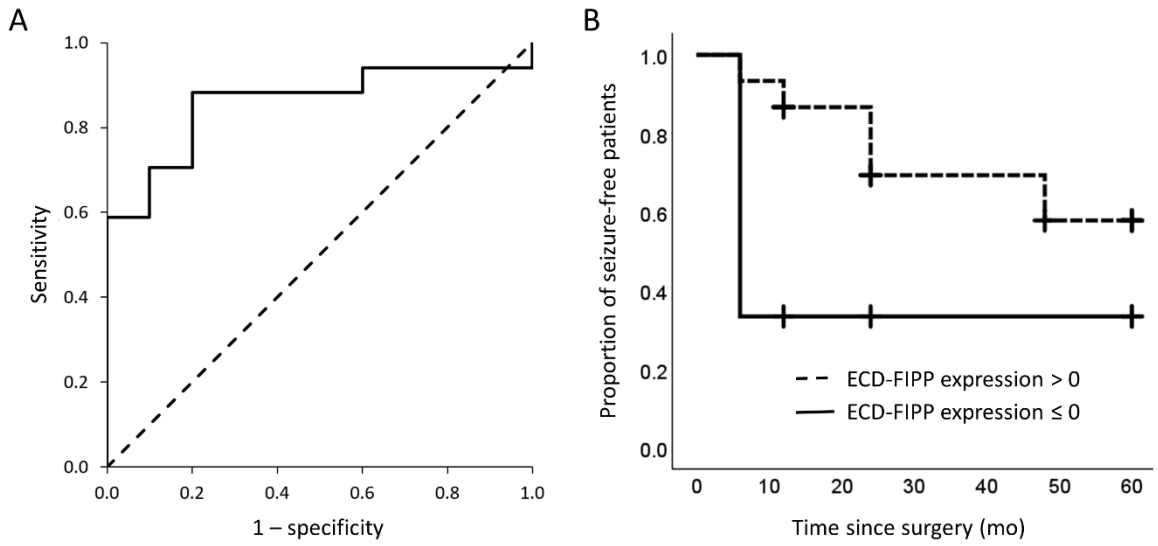

SUPPLEMENTAL FIGURE 5 ROC analysis of the ECD-FIPP expression score for identification of responders in the ^{99m}Tc-ECD subsample (A), and Kaplan-Meier analysis of patients with positive ECD-FIPP expression score versus patients with negative ECD-FIPP expression score (B).

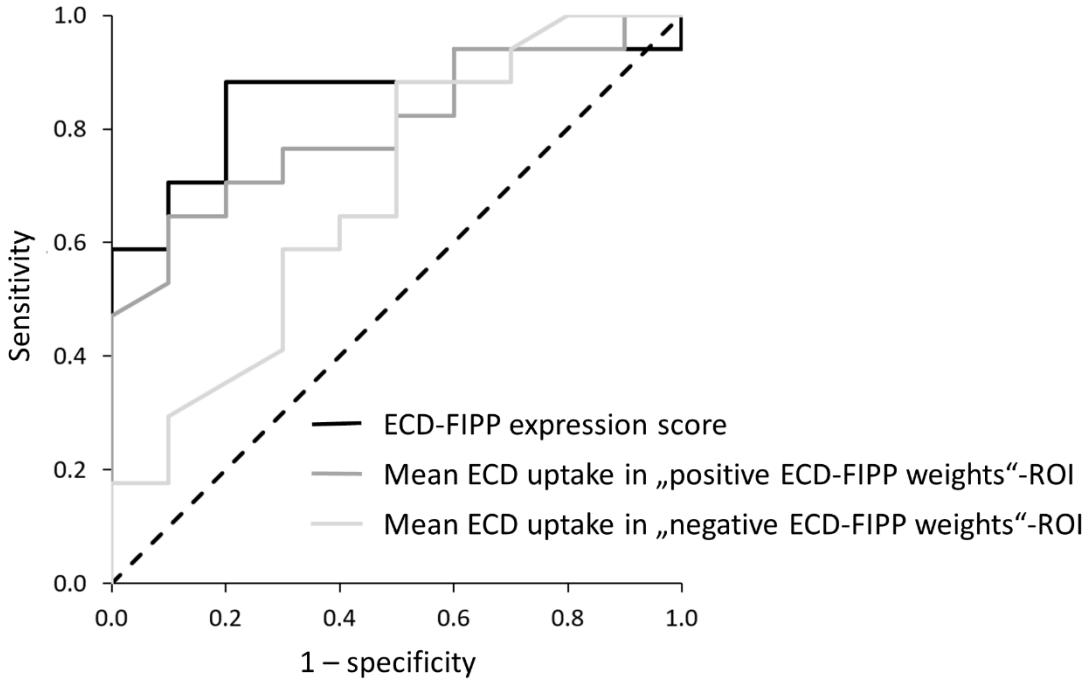

SUPPLEMENTAL FIGURE 6 ROC analysis for the identification of responders in the ^{99m}Tc-ECD subsample by the mean ^{99m}Tc-ECD uptake in the “positive ECD-FIPP weights”-ROI and in the “negative ECD-FIPP weights”-ROI. The ROC curve of the ECD-FIPP expression score is shown for comparison.

SUPPLEMENTAL TABLE 1 Demographical, clinical, SPECT and surgical data of the subsample with ^{99m}Tc-ECD brain perfusion SPECT

	responder*	**non-responder***	***P*†**
number of patients	17	10	
sex [% females]	40	41	1.00
age at ictal SPECT [y]	42 [27-46]	29 [23-45]	0.19
age at first seizure [y]	13 [6-23]	13 [5-23]	0.90
duration of disease at ictal SPECT [y]	23 [13-35]	20 [11-26]	0.39
mean seizure frequency in the last 12 months before ictal SPECT [seizures/month]	8 [3-21] (n=14)	14 [7-16] (n=8)	0.44
with impairment of awareness in the majority of seizures during the last 12 months [%]	75 (n=12)	88 (n=8)	0.62
lateralization of seizure semiology: ipsilateral to resection/contralateral/both/no [%]	92/8/0/0 (n=13)	100/0/0/0 (n=6)	1.00
lateralization of MRI: ipsilateral to resection/contralateral/both/no [%]	94/0/0/6	89/0/0/11 (n=9)	1.00
lateralization of ictal EEG prior to ictal SPECT: ipsilateral to resection/contralateral/both/no [%]	87/7/7/0 (n=15)	89/0/0/11 (n=9)	0.41
lateralization of interictal EEG prior to ictal SPECT: ipsilateral to resection/contralateral/both/no [%]	82/6/12/0	60/0/30/10	0.28
^{99m}Tc-ECD activity administered for ictal SPECT [MBq]	523 [472-615]	590 [462-737]	0.41
latency of ^{99m}Tc-ECD injection to seizure start in EEG [s]	31 [27-35]	33 [25-46]	0.41
seizure duration after injection according to EEG [s]	78 [42-147]	76 [38-182]	0.86
delay of surgery after ictal SPECT [months]	12 [4-32]	6 [3-71]	0.71
side of TLE surgery [% right]	65	70	1.00
neuropathology of surgical specimen: normal/sclerosis/mass lesion/focal cortical dysplasia	13/80/7/0 (n=15)	20/40/40/0 (n=5)	0.15

*Continuous variables are given as median [interquartile range]. If a variable was not available in all patients, the number of patients for that variable is given in parentheses.

†The P-values are not corrected for multiple testing.